ARTICLE

Glyphosate sensing in aqueous solutions by fluorescent zinc(II) complexes of [9]aneN$_3$-based receptors†

Received 00th January 20xx,

Accepted 00th January 20xx

DOI: 10.1039/x0xx00000x

Alessandra Garau,*[a] Giacomo Picci,[a] Andrea Bencini,*[b] Claudia Caltagirone,[a] Luca Conti,[b] Vito Lippolis, [a] Paola Paoli,[c] Giammarco Maria Romano, [b] Patrizia Rossi,[c] Mariano Andrea Scorciapino.[a]

Herein we describe the binding abilities of Zn(II) complexes of [12]aneN$_4$- (**L1)** and [9]aneN$_3$-based receptors (**L2**, **L3**) towards the herbicides N-(phosphonomethyl)glycine (glyphosate, H$_3$PMG) and 2-amino-4-[hydroxy(methyl)phosphoryl]butanoic acid (glufosinate, H$_2$GLU), and also aminomethylphosphonic acid (H$_2$AMPA), the main metabolite of H$_3$PMG, and phosphate. All ligands form stable Zn(II) complexes, whose coordination geometries allow a possible interaction of the metal center with exogenous anionic substrates. Potentiometric studies evidenced the marked coordination ability of the **L2**/Zn(II) system for the analytes considered, with a preferential binding affinity for H$_3$PMG over the other substrates, in a wide range of pH. ^{1}H and ^{31}P NMR experiments supported the effective coordination of such substrate by the Zn(II) complex of **L2**, while fluorescence titrations and test strip were performed to evaluate whether the H$_3$PMG recognition processes could be detected by fluorescence signaling.

Introduction

N-(phosphonomethyl)glycine, generally called glyphosate and herein indicated as H$_3$PMG, is a non-selective and broad-spectrum organophosphorus herbicide extensively used worldwide for systemic weeds control both on arboreal and herbaceous crops and on areas not destined to agricultural crops, such as industrial and civil areas, embankments and roadsides.[1-5] Overuse of glyphosate has released a large amount of residues into soil and drinking water[6,7] and the greatest risk of water contamination comes from urban areas with larger paved surfaces where rain washes this substance into receiving channels. On the other hand, glyphosate dispersed in fields, forests and other types of soil by spraying, has low penetration properties because it remains stationary in the upper layers of soil where it is degraded by bacteria without reaching groundwater. Microbial degradation of H$_3$PMG produces its main metabolite, aminomethylphosphonic acid (H$_2$AMPA). H$_2$AMPA is highly soluble in water with a consequent greater risk of transfer to groundwater maintaining at the same time a significant biological activity comparable to that of glyphosate.[8] Glyphosate can irreversibly inactivate acetylcholinesterase (AChE) to cause different adverse physiological reactions, which might cause respiratory, myocardial, and neuromuscular dysfunctions.[6,9-11] Furthermore, recent studies have indicated that glyphosate is potentially carcinogenic to humans[12] although there are conflicting opinions on its carcinogenicity between the US Environmental Protection Agency (EPA) and the International Agency for Research on Cancer (IARC).[13] The EPA has set to 4.1 µM the maximum contaminant level (MCL) of glyphosate in drinking water.[9-14] Finally, 2-amino-4-[hydroxy(methyl)phosphoryl]butanoic acid (H$_2$GLU, generally called glufosinate) is a broad-spectrum and fast acting herbicide used to manage glyphosate-resistant weeds mainly because of its broad-spectrum action mode.[15] Although its use has increased exponentially over the past decade, the areas treated with this herbicide are far less than that treated with glyphosate, due to its less efficiency against weeds. Differently form H$_3$PMG, H$_2$GLU targets glutamine synthetase, and its adverse activity has recently been attributed to the formation of reactive oxygen species (ROS), followed by lipid peroxidation.[16] Glufosinate would disrupt both photorespiration and the light reactions of photosynthesis, leading to photoreduction of molecular oxygen, which generates ROS. Its proper use is considered safe, but concerns regarding its ecotoxicology are arising.[17]

In recent years, different techniques have been developed for the monitoring and the detection of such important substrates in environmental matrices, including high performance liquid chromatography (HPLC),[18,19] gas chromatography-mass spectrometry (GC-MS),[20] ion chromatography (IC),[21] capillary electrophoresis (CE),[22] enzyme-linked immunosorbent assays (ELISA)[23] and optical[24] and electrochemical immuno-assays.[25-27] Most of these methods require expensive equipment and complex procedures, thus other methodologies have been developed to detect glyphosate, based on optical measurements, in particular fluorescence that are highly sensitive, much simpler to operate, cost-effective, and rapid. Most of the reported fluorescent systems are based on quantum dots, nanoclusters, metalorganic frameworks, but also fluorescent molecular probes featuring coumarin, rhodamine and benzothiazole as fluorogenic moieties are known. Generally, the mechanism of detection of glyphosate by fluorescent chemosensors is based on the supramolecular sensing paradigm of the displacement assay.[28,29] Interestingly, there are very few optical

[a] Dipartimento di Scienze Chimiche e Geologiche, Università degli Studi di Cagliari, S.S. 554 Bivio per Sestu, 09042, Monserrato, Cagliari (Italy)E-mail: agarau@unica.it.

[b] Dipartimento di Chimica 'Ugo Schiff', Università degli Studi di Firenze, Via della Lastruccia 3, 50019 Sesto Fiorentino, Firenze (Italy)

[c] Dipartimento Ingegneria Industriale, Università degli Studi di Firenze, Via Santa Marta 3, Firenze 50139 (Italy)

†Electronic Supplementary Information (ESI) available: CCDC 2154815. See DOI: 10.1039/x0xx00000x

chemosensors based on metal complexes in which the recognition/sensing process of glyphosate occur through metal binding.[29c]

The design and development of fluorescent artificial receptors able to selectively recognise and sense targeted anionic species, has increased considerably in recent years becoming a prominent and active field of research within the frame of SupramolecularChemistry in the relatively young area of anion coordination chemistry.[28-34]

As compared to metal ions, when it comes to the design artificial receptors at molecular level, the coordination chemistry of anionic species presents different additional factors to consider such as larger size and a variety of shapes for the anions, higher hydration energies within a wide scale of hydrophobicity and limited pH range of existence due to possible protonation process in water-containing solutions. To this purpose, two of the most adopted synthetic strategies are based either on non-covalent intermolecular weak interactions (H-bonding, π-stacking and electrostatic interactions and hydrophobic effects) *via* topological complementarity of the receptors, or on metal-ligand covalent interactions with metal complex hosts where the metal cation and the organic ligand can both bind and sense the targeted anionic species. For both strategies, acyclic and cyclic polyamine ligands, particularly 1,4,7-triazacyclononane ([9]aneN$_3$) and 1,4,7,10-tetraazacyclododecane ([12]aneN$_4$, cyclen), have largely been employed.[35,36] Selective recognition or optical sensing of anions can be obtained by tuning the ligand structure through the functionalization of the NH groups with pendant arms having different coordinating units and functions to obtain an appropriate optimization between the anchoring/pre-organizing ability of the coordinated metal and the binding properties of the ligand functions *via* non-covalent interactions.

The [9]aneN$_3$ and [12]aneN$_4$ derivatives considered in the present study are reported in Scheme 1.[37-39] In all cases, quinoline is used as fluorogenic fragment(s) linked to the cyclic frameworks *via* a methylene bridge (**L1**) or an amide function(s) (**L2** and **L3**). As previously described, **L2** and **L3** exhibit an optical response towards Zn(II) *via* an OFF-ON Chelation Enhancement of the Fluorescence Emission (CHEF) effect in MeCN/H$_2$O (1:4 v/v at pH = 7.4 MOPS buffer) following metal complexation.[37a,38] In both cases the coordination of the carbonyl group from the pendant arm(s) has been proposed at the origin of the observed optical response. In both Zn(II) complexes of **L2** and **L3**, the coordination sphere of the metal is not saturated by the ligand donors, making them potential metal-based receptors for anionic species, for which changes in the optical properties could be envisaged in consequence of the host-guest interaction. Differently from **L2** and **L3**, **L1** features a tetraamine macrocyclic unit and the quinoline nitrogen atom is close to the macrocyclic unit, so all five nitrogen atoms could participate to metal binding. However, Zn(II) could expand its coordination sphere, achieving hexa-coordination in the presence of a coordinating exogenous ligand; therefore, also the Zn(II) complex with **L1** might be a potential receptor for exogenous substrates.

For this reason, we decided to study the behaviour of the Zn(II) complexes with **L1-L3** towards different substrates, particularly glyphosate (H_3PMG), aminomethylphosphonic acid (H_2AMPA) glufosinate (H_2GLU), and phosphate (Scheme 1).

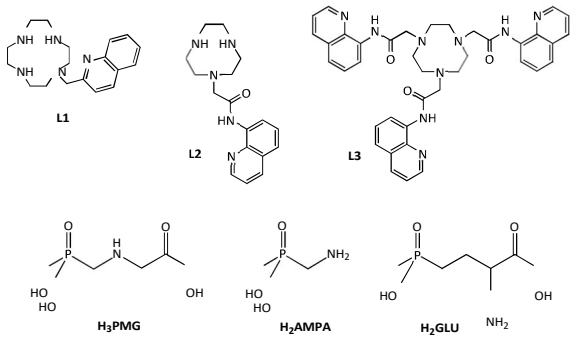

Scheme 1. Cyclic polyamine derivatives and targeted analytes considered in this paper.

Results and discussion

While Zn(II) coordination with **L2** and **L3** has previously been reported,[37a,38] no analysis of the binding characteristic of **L1** for this metal has yet been reported. Therefore, we first investigated Zn(II) binding with **L1** in solution by coupling potentiometric, UV-Vis and fluorescence emission measurements.

Zn(II) complexation with L1. The analysis of the Zn(II) coordination with **L1**, carried out in MeCN/H$_2$O (1:4 v/v) solution by potentiometric titrations, requires preliminary determination of the protonation constants of the ligand in the same medium. The observed values are reported in Table 1, together with the Zn(II) complexes formed by **L1** and their formation constants, while in Figure S1 (Electronic Supporting Information, ESI†) the distribution diagrams of the species formed in solution are reported. The protonation constants are quite similar to those determined in water in a previous study,[39] and account for the protonation of the macrocyclic ring in the first two protonation steps, while the quinoline nitrogen atom results to protonate in the last protonation step occurring at acidic pH values. Zn(II) gives a stable 1:1 complex with **L1** in solution, in which the metal is likely coordinated by the four amine group of the [12]aneN$_4$ moiety. Furthermore, the quinoline nitrogen atom is nicely placed to participate in metal coordination, thus affording a penta-coordinated Zn(II) ion.

Table 1. Protonation and Zn(II) complexation constants of **L1** in MeCN/H$_2$O (1:4 v/v) (NMe$_4$Cl 0.1 M, 298.1 K).

Equilibria	log*K*
L1 + H^+ = [H**L1**]$^+$	10.24 (4)
[H**L1**]$^+$ + H^+ = [H_2**L1**]$^{2+}$	9.53 (5)
[H_2**L1**]$^{2+}$ + H^+ = [H_3**L1**]$^{3+}$	2.64 (4)
L1 + Zn^{2+} = [Zn**L1**]$^{2+}$	15.80 (5)
[Zn**L1**]$^{2+}$ + H^+ = [ZnH**L1**]$^{3+}$	3.80 (4)
[Zn**L1**]$^{2+}$ + OH^- = [Zn**L1**(OH)]$^+$	3.86 (6)

Participation of the heteroaromatic nitrogen to metal binding is also suggested by UV-Vis spectra recorded for a solution of **L1** in the presence of increasing amounts of Zn(II) at pH 7 (TRIS buffer). The spectra show in the range 300-320 nm the typical structured band of a quinoline moiety, whose absorption increases with the addition of Zn(II) (Figure 1).

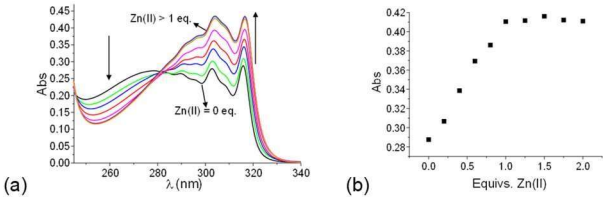

Figure 1. (a) UV-Vis spectra and (b) absorbance at 316 nm of **L1** in MeCN/H_2O (1:4 v/v) at pH 7 (TRIS buffer) in the presence of increasing amounts of Zn(II) ([**L1** = 1.0 × 10^{-5} M]).

The absorption monitored at 316 nm linearly increases up to a Zn(II)/**L1** molar ratio (R) of 1 to achieve a constant value for R > 1. This result confirms the formation of a stable 1:1 Zn(II)/**L1** complex, in which the quinoline moiety is involved in the metal ion coordination. Considering the fluorescence emission of **L1**, the ligand is almost not emissive at pH 7 (TRIS buffer) in MeCN/H_2O (1:4 v/v). As often found for Zn(II) complexes of polyamine ligands bearing quinoline pendant arms,[37a,38] metal complexation by **L1** induces an enhancement of the emission of the quinoline fluorophore (CHEF effect). As shown in Figure 2, addition of Zn(II) to a solution of **L1** buffered at pH 7 (TRIS buffer), leads to the appearance of the typical broad emission band of the quinoline moiety at 380 nm. The emission increases upon Zn(II) addition up to a 0.9 metal-to-ligand molar ratio (R), accompanied by a slight blue-shift of the band, while no significant changes in the spectra are observed for R > 1.1. Once again, this observation accounts for the formation of a stable 1:1 complex with Zn(II)/**L1**, likely involving coordination of the quinoline nitrogen atom to the metal.

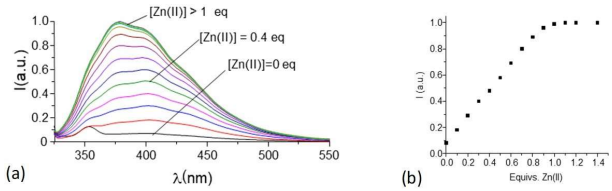

Figure 2. (a) Fluorescence emission spectra and (b) emission intensity at 380 nm of **L1** in MeCN/H_2O (1:4 v/v) at pH 7 (TRIS buffer) in the presence of increasing amounts of Zn(II) ([**L1** = 1.0 × 10^{-5} M], λ_{exc} = 295 nm).

Crystals of the Zn(II) complex with **L1** were also isolated and the X-ray crystal structure solved. In the asymmetric unit of [Zn**L1**](ClO_4)$_2$·0.25H_2O the [Zn**L1**]$^{2+}$ cation, two disordered perchlorate anions and 0.25 molecules of co-crystallized water are present.

As expected, the zinc(II) cation is penta-coordinated by the four nitrogen atoms from the macrocyclic unit and by the nitrogen atom from the quinoline moiety (Figure 3), with the zinc atom being 0.7238(9) Å out of the mean plane defined by the nitrogen atoms N1, N2, N3 and N4. The resulting coordination polyhedron may be described as a distorted square pyramid. The Zn-N distances 2.017(5)-2.158(5) Å (the distance with the apical N5 atom being the shortest) are in agreement with those retrieved in the Cambridge Structural database (CSD, v. 5.42) for similar Zn(II) complexes. For instance, strict analogies can be found in the Zn(II) complex with ligand 6-((1,4,7,10-tetraazacyclododecyl)methyl)uracil (Refcode = RUHWIA, see Figure S2, ESI).[40]

Figure 3. View of the structure of the [Zn**L1**]$^{2+}$ cation in [Zn**L1**](ClO$_4$)$_2$·0.25H$_2$O with labelling scheme adopted. Displacement ellipsoids are drawn at 30% probability level. Hydrogen atoms, counter-anions and co-crystallized water molecules are not reported for the sake of clarity. Bond distances (Å) and angles (°) are reported in Table S1 in the ESI.

Concerning the overall shape of the coordinated **L1** ligand, the [12]aneN$_4$ ring adopts the usual [3333] corner conformation while the quinoline ring is almost perpendicular to it. The angle between the mean plane defined by the non-hydrogen atoms of the quinoline and that defined by the nitrogen atoms of the [12]aneN$_4$ ring is 78.6(1)°.

Binding of the target species by the Zn(II) complexes of L1, L2 and L3. To analyse the binding features of the Zn(II) complexes of **L1**, **L2** and **L3** towards the analytes under investigation, we performed potentiometric titrations in order to determine the species formed in solution and their stability constants and to point out the possible selectivity patterns among the different substrates. As previously reported, in MeCN/H_2O (1:4 v/v), **L2** and **L3** form stable Zn(II) complex with a 1:1 metal-to-ligand stoichiometry in the pH range 5-7.[37a,38] In the case of **L3**, the formation of a less stable Zn(II) complex with a metal-to-ligand 1:2 stoichiometry is also observed. In the course of the present work, we preliminarily determined the protonation constants of the analytes (H_3PMG, H_2AMPA, H_2GLU, phosphate) and the stability constants of their Zn(II) complexes in the same medium (MeCN/H_2O 1:4 v/v). Their values are summarized in Table S2, while Scheme S1 reports sketches of the different protonated forms of the substrates.

The determined protonation and Zn(II) binding constants of H_3PMG and H_2AMPA are similar to those previously reported in aqueous solution.[41-44] This also applies to the protonation constants H_2GLU,[45] while the formation constant of its Zn(II) complex has not been reported in previous studies neither in water or in other solvents. H_3PMG, H_2AMPA and H_2GLU feature a rather high constant for their first protonation equilibrium (A + H^+ = AH^+), ranging from 9.85(3) (A = GLU^{2-}) to 10.43(1) (A = PMG^{3-}), which is normally attributed to protonation of the amine group.[41-45] The second protonation constant is lower than 7 log units and proton binding, which occurs on the phosphonate ($HPMG^{2-}$, $HAMPA^-$)[41-44] or phosphinate ($HGLU^-$)[45] groups, takes place in the acidic pH region. As a consequence, in a large pH region, including neutral pH, the main species present in solution are the monoprotonated zwitterionic forms $HPMG^{2-}$, $HAMPA^-$ and $HGLU^-$. Finally, in the case of H_3PMG a third protonation equilibrium is observed below pH 3 and involves the acetate group. Among the different analytes, PMG^{3-} displays the better binding ability for 'free' Zn(II) ion, as expected considering the higher charge of the anion and the possible use of its three binding groups for metal binding.[41-43] On the other hand, the binding constant of Zn(II) for **L2** (the worst chelating agent among the **L1-L3** ligands) is *ca.* two order of magnitude greater than the corresponding binding constant of PMG^{3-} (log *K* = 11.79(4) and 9.69(3) for Zn(II) complexation with **L2** and PMG^{3-}, respectively). This

would suggest that in the presence of these analytes, the Zn(II) complexes with **L1**-**L3** cannot undergo trans-metallation reactions. This suggestion is confirmed by ESI mass spectra recorded on solutions containing Zn(II) and **L2** in equimolecular ratio at pH 7 in the absence and in the presence of H_3PMG. Indeed, the spectrum obtained in the absence of the analyte shows a peak with m/z at 376.1091, attributable to a positively charged $[Zn\mathbf{L2}]^+$ complex (Figure S3, ESI). In the presence of large excess of glyphosate at pH 7 (up to 10 equiv. with respect to the ligand **L2**, Figure S3b), the mass spectrum does not show any peak attributable to glyphosate adducts with the Zn(II) complex of **L2**, but the peak of the $[Zn\mathbf{L2}]^{2+}$ is clearly observable. This result corroborates the hypothesis that the anionic substrate is not able to induce demetallation of the Zn(II) complex with **L2** at neutral pH.

Finally, we also analysed the possible interaction of the protonated forms of **L1-L3** with the analytes under investigation. In the absence of Zn(II), no interaction is detected between the receptors and the anionic forms of the analytes, with the only exception of **L1**, for which a weak interaction between the mono- and diprotonated forms, $H\mathbf{L1}^+$ and $H_2\mathbf{L1}^{2+}$ and the $HPMG^{2-}$ anion is found (Table 2).

Considering the interaction of the analytes with the Zn(II) complexes of **L1**-**L3**, in the case of **L2** and **L3** precipitation was observed in the alkaline pH region in the course of the potentiometric titrations in the presence of Zn(II), probably due to the formation of insoluble ternary complexes, preventing the speciation studies above pH 8. In the case of the Zn(II) complex with **L3** in the presence of H_3PMG, precipitation takes place above pH 6, and therefore, the speciation analysis of this system was limited to the acidic pH region. Tables 2-4 report the formation constants of the ternary adducts of the Zn(II) complexes with ligands **L1**, **L2** and **L3** and the analytes considered. Distributions diagrams for the species formed are reported in Figures 4 (**L2**) and S4 and S5 (**L1** and **L3**, respectively, ESI†).

As normally observed for the interaction of anionic substrates to charged metal complexes, for a given analyte, the addition constants to the $[Zn\mathbf{L}]^{2+}$ complex (**L** = **L1**, **L2** or **L3**) increase with the negative charge gathered on the analyte, likely due to the increasing electrostatic interaction between the metal ion and the substrates. As shown in Figures 4, S4 and S5 for **L2**, **L1** and **L3**, respectively, the most abundant complexed species present in solution at neutral pH values are the ternary adducts $[Zn\mathbf{L}(HA)]^{(n-2)-}$ [A = PMG^{3-}, $AMPA^{2-}$ and GLU^{2-}, **L** = **L1**, **L2** or **L3**, n = 1 ($AMPA^{2-}$ and GLU^{2-}) or 2 (PMG^{3-})], in which the anionic substrate is in its monoprotonated form. More interestingly, the data in Tables 2-4 outline that for all analytes under investigation, the binding ability increases in the order $[Zn\mathbf{L1}]^{2+}$ < $[Zn\mathbf{L3}]^{2+}$ < $[Zn\mathbf{L2}]^{2+}$. This sequence can be evidenced comparing the addition constants of the four different substrates with the same protonation degree and negative charge to $[Zn\mathbf{L}]^{2+}$ complexes. For instance, the addition constants of $HPMG^{2-}$ to the $[Zn\mathbf{L1}]^{2+}$, $[Zn\mathbf{L3}]^{2+}$ and $[Zn\mathbf{L2}]^{2+}$ complexes are 3.14(5), 4.40(7) and 5.55(3) log units, respectively. The different coordination ability displayed by the three analytes could be related to the coordination sphere of Zn(II) in its complexes with **L1-L3**. The crystal structure of the $[Zn\mathbf{L1}]^{2+}$ complex shows that the metal is coordinated by the four amine groups of the macrocyclic unit and the quinoline nitrogen atom. In the case of $[Zn\mathbf{L2}]^{2+}$, it was found that the metal is basically coordinated by the three amine functions of the [9]aneN$_3$ unit; however, the carbonyl oxygen of the amide moiety is also involved in metal coordination.[38] Similarly, in the case of $[Zn\mathbf{L3}]^{2+}$ the [9]aneN$_3$ macrocycle is the main binding unit, while the carbonyl oxygen of two amide functions are also involved in metal binding.[37a] These different coordination environments also justify the different stability of the Zn(II) complex with the three receptors in solution. In fact, the stability constant of the $[Zn\mathbf{L}]^2$ species decreases in the order **L1** > **L3** > **L2** (log *K* = 15.80(5), 13.1(1) and 11.79(4) log units for **L** = **L1**, **L3** and **L2**, respectively). The higher binding ability for the four anionic analytes displayed by the $[Zn\mathbf{L2}]^{2+}$ complex is reasonably due to the coordination environment of the metal ion, which is less saturated by the ligand donors. Conversely, the $[Zn\mathbf{L1}]^{2+}$ complex, in which the metal is firmly bound by the tetra-azamacrocyclic moiety and the heteroaromatic nitrogen donor, shows the lower binding affinity for all substrates among the three ligands.

Table 2. Formation constants of the complexes of H_3PMG with the protonated forms of **L1**, and addition constants of H_3PMG, H_2AMPA, H_2GLU and phosphate to the $[Zn\mathbf{L1}]^{2+}$ complex in MeCN/H_2O (1:4 v/v) (NMe_4Cl 0.1 M, 298.1 K).

Equilibria	log *K*
$H\mathbf{L1}^+ + HPMG^{2-} = [H\mathbf{L1}(HPMG)]^-$	1.95 (7)
$H_2\mathbf{L1}^{2+} + HPMG^{2-} = [H_2\mathbf{L1}(HPMG)]$	2.35 (8)
$[Zn\mathbf{L1}]^{2+} + GLU^{2-} = [Zn\mathbf{L1}(GLU)]$	4.20 (3)
$[Zn\mathbf{L1}]^{2+} + HGLU^- = [Zn\mathbf{L1}(HGLU)]^+$	3.14 (9)
$[Zn\mathbf{L1}]^{2+} + PMG^{3-} = [Zn\mathbf{L1}(PMG)]^-$	4.16 (6)
$[Zn\mathbf{L1}]^{2+} + HPMG^{2-} = [Zn\mathbf{L1}(HPMG)]$	3.14 (5)
$[Zn\mathbf{L1}]^{2+} + AMPA^{2-} = [Zn\mathbf{L1}(AMPA)]$	3.30 (8)
$[Zn\mathbf{L1}]^{2+} + HAMPA^- = [Zn\mathbf{L1}(HAMPA)]^+$	3.08 (2)
$[Zn\mathbf{L1}]^{2+} + HPO_4^{2-} = [Zn\mathbf{L1}(HPO_4)]$	2.65 (8)

Table 3. Addition constants H_3PMG, H_2AMPA, H_2GLU and phosphate to the $[Zn\mathbf{L2}]^{2+}$complex in MeCN/H_2O (1:4 v/v) (NMe_4Cl 0.1 M, 298.1 K).

Equilibria	log *K*
$[Zn\mathbf{L2}]^{2+} + HPMG^{2-} = [Zn\mathbf{L2}(HPMG)]$	5.55 (3)
$[Zn\mathbf{L2}]^{2+} + H_2PMG^- = [Zn\mathbf{L2}(H_2PMG)]^+$	4.82 (4)
$[Zn\mathbf{L2}]^{2+} + HAMPA^- = [Zn\mathbf{L2}(HAMPA)]^+$	3.50 (3)
$[Zn\mathbf{L2}]^{2+} + H_2AMPA = [Zn\mathbf{L2}(H_2AMPA)]^{2+}$	3.01 (4)
$[Zn\mathbf{L2}]^{2+} + GLU^{2-} = [Zn\mathbf{L2}(GLU)]$	4.40 (3)
$[Zn\mathbf{L2}]^{2+} + HGLU^- = [Zn\mathbf{L2}(HGLU)]^+$	3.83 (4)
$[Zn\mathbf{L2}]^{2+} + HPO_4^{2-} = [Zn\mathbf{L2}(HPO_4)]$	3.41 (6)
$[Zn\mathbf{L2}]^{2+} + H_2PO_4^- = [Zn\mathbf{L2}(H_2PO_4)]^+$	1.91 (9)

Table 4. Addition constants of H_3PMG, H_2AMPA, H_2GLU and phosphate to the $[Zn\mathbf{L3}]^{2+}$ complex in MeCN/H_2O (1:4 v/v) (NMe_4Cl 0.1 M, 298.1 K).

Equilibria	log *K*
$[Zn\mathbf{L3}]^{2+} + HPMG^{2-} = [Zn\mathbf{L3}(HPMG)]$	4.40 (7)
$[Zn\mathbf{L3}]^{2+} + H_2PMG^- = [Zn\mathbf{L3}(H_2PMG)]^+$	3.83 (8)
$[Zn\mathbf{L3}]^{2+} + HAMPA^- = [Zn\mathbf{L3}(HAMPA)]^+$	3.23 (7)
$[Zn\mathbf{L3}]^{2+} + H_2AMPA = [Zn\mathbf{L3}(H_2AMPA)]^{2+}$	2.84 (6)
$[Zn\mathbf{L3}]^{2+} + HGLU^- = [Zn\mathbf{L3}(HGLU)]^+$	3.65 (9)
$[Zn\mathbf{L3}]^{2+} + H_2GLU = [Zn\mathbf{L3}(H_2GLU)]^{2+}$	3.12 (7)
$[Zn\mathbf{L3}]^{2+} + H_2PO_4^- = [Zn\mathbf{L3}(H_2PO_4)]^+$	2.16 (9)

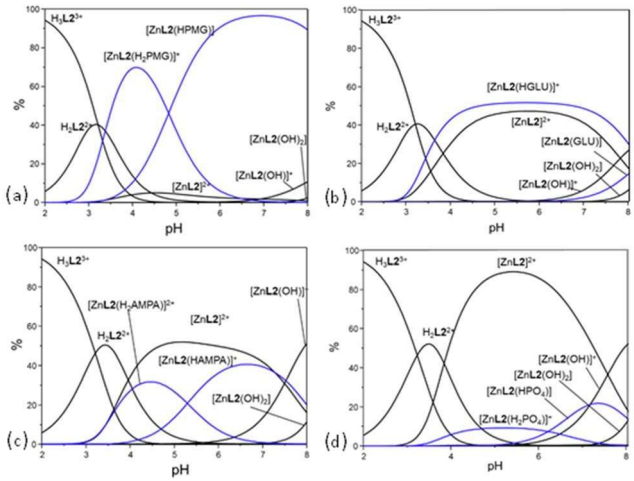

Figure 4. Distribution diagrams of the complexes formed in a system containing **L2**, Zn(II) and H_3PMG) (a), H_2GLU (b) H_2AMPA) (c) and phosphate (d), in 1:1:1 molar ratio in $MeCN/H_2O$ (1:4 v/v) (NMe_4Cl 0.1 M, 298 K [**L2**] = 1.0×10^{-3} M]).

Considering the binding affinity of the different substrates to the Zn(II) metal complexes, a comparison between the addition constants of the analytes with the same negative charge to each $[Zn\mathbf{L}]^{2+}$ complex cation (**L** = **L1**, **L2**, or **L3**) would suggest that glyphosate forms the most stable adducts with the Zn(II) complexes, with **L2** and **L3**, which, in turn, give weaker interactions with glufosinate, aminophosphonate and phosphate. For instance, the addition constants of H_2PMG^-, $HGLU^-$, $HAMPA^-$ and $H_2PO_4^-$ to the $[Zn\mathbf{L2}]^{2+}$ complex are 4.82(4), 3.83(4), 3.50(3) and 1.91(9) log units, respectively. In the case of the $[Zn\mathbf{L1}]^{2+}$, glufosinate appears to form slightly more stable ternary adduct than glyphosate. Of note, in the case of $[Zn\mathbf{L2}]^{2+}$ with $HPMG^{2-}$ there is a wide pH window in which the ternary species [Zn**L2**(HPMG)] is the prevailing species present in solution (Figure 4a). However, the analysis of the selectivity properties of a receptor toward different analytes by using the simple comparison of the stability constants of the complexes can be sometimes misleading, due to the presence in solution of multiple equilibria involving different protonated species of the analytes, whose presence is strictly related to the pH of the aqueous medium. The selectivity properties of the three Zn(II) complexes can be optimally visualized by considering a competitive systems containing the ligand, Zn(II), and all four substrates in equimolecular concentrations and calculating the overall percentages of the different adducts formed over a wide pH range.[46] Similar selectivity plots are shown in Figure 5 for the Zn(II) complexes with **L1**, **L2** and **L3**, respectively.

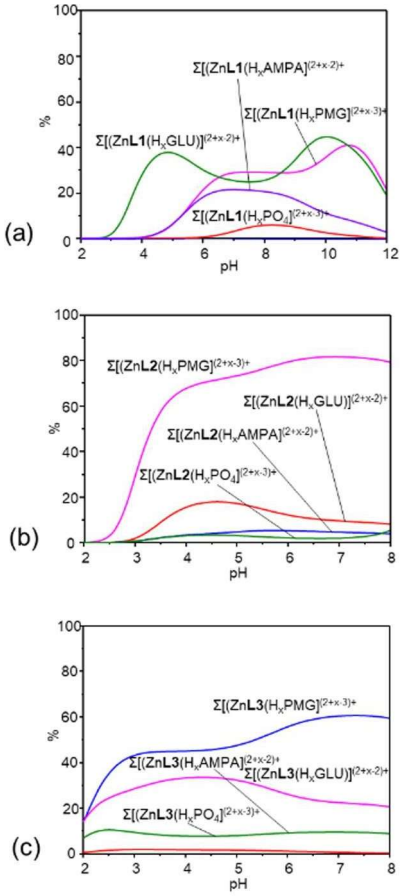

Figure 5. Plots of the overall percentages of H_3PMG, H_2GLU, H_2AMPA and phosphate complexed by the 1:1 Zn(II) complexes with **L1** (a), **L2** (b) and **L3** (c) *versus* pH in $MeCN/H_2O$ 1:4 v/v ([**L**] = [Zn(II)] = [H_3PMG] = [H_2GLU] = [H_2AMPA] = [phosphate] = 1.0×10^{-3} M, **L** = **L1**, **L2** or **L3,**) NMe_4Cl 0.1 M, 298.1 K). The overall percentages of not-complexed substrates, Zn(II) and ligands have been not reported for clarity.

Figure 5b points out that the Zn(II) complex with **L2** possesses a remarkable selectivity for H_3PMG over the other analytes over a wide pH range, including pH 7. A similar behaviour is also found in **L3**, although in this case preferential binding of H_3PMG is less marked (Figure 5c). Selectivity is lost in the case of **L1**, where the ternary adducts with H_3PMG and H_2GLU are formed in similar percentages at neutral and alkaline pH values, while the ternary complexes with H_2GLU are prevalent in solution below pH 6 (Figure 5a).

In order to obtain atomistic level details about the most stable ternary adduct, which is formed by $[Zn\mathbf{L2}]^{2+}$ and H_3PMG, we recorded a series of ^1H NMR spectra in CD_3CN/D_2O solution (Figure 6).

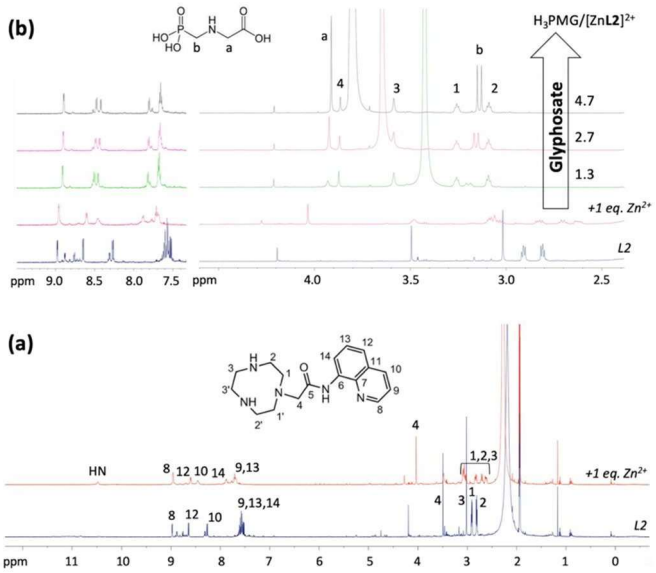

Figure 6. (a) The full ^{1}H NMR spectrum of **L2** is compared to that recorded after the addition of 1 equiv. of Zn(II) in CD_3CN solution. (b) Two regions of interest of the same spectra are shown and compared with those obtained upon progressive addition of a water solution of glyphosate as indicated by the arrow ($H_3PMG/[ZnL2]^{2+}$ molar ratio is also indicated). The Lewis structure of **L2** and glyphosate are shown with numbers and lowercase letters, respectively, to label the corresponding resonances.

The ^{1}H NMR spectrum of **L2** noticeably changes upon addition of 1 equiv. of Zn(II). Detailed discussion has been reported elsewhere,[38] but it is important to recall the attention on the resonances of the macrocycle's protons. In the absence of Zn(II), an almost canonical first order spin system is observed, with two clear triplets accounting for all the protons labelled with 1 and 2 in Figure 6 and one singlet for the protons 3. This is a clear fingerprint for the macrocycle with negligible conformational constraints in solution. On the other hand, the coordination of the Zn(II) results into the macrocycle being locked in a rigid conformation. This becomes clear in the ^{1}H NMR spectrum as the spin system changes into second order and a series of complex multiplets correspondingly appears in the aliphatic region. Interestingly, the ^{1}H NMR spectrum turns back to first order upon addition of the H_3PMG to the solution, which is a clear indication that the interaction of the macrocyclic amine groups with the metal becomes weaker upon coordination of the substrate to Zn(II) and, consequently, the macrocycle partially recovers its conformational flexibility. Nonetheless, the two triplets and the singlet assigned to macrocyclic protons are significantly shifted and broadened, when compared with the spectrum of the free **L2**. This suggests that flexibility is not completely recovered and, thus, **L2** is not free but retains coordination to Zn(II). Finally, both resonances of glyphosate progressively shift with increasing concentration, suggesting the interaction of this analyte with the $[ZnL2]^{2+}$ complex. In particular, the methylene labelled as b in Figure 6b, whose resonance is a doublet by virtue of scalar coupling with the ^{31}P, exhibits the most significant shift, clearly indicating that the interaction between the glyphosate and the complex is due to the phosphate group. The corresponding proton-decoupled ^{31}P NMR spectra bolster this evidence. Upon addition of glyphosate, the single H_3PMG resonance, although its chemical shift changes only slightly, shows a significant broadening (Figure S6, ESI†), which is a clear indication of a change in the spin-spin relaxation time (T_2^*). This is probably due to chemical exchange between the free and the bound form of glyphosate in solution.

The progressive shift towards higher frequency of the residual water resonance that accompanied the acetonitrile signal (Figure 6), is related to the progressive increase of water amount in the mixture during the titration. Finally, we compared the molecular potential energy (at a classical level) of two possible $[ZnL2]^{2+}$ adducts with glyphosate, formed by one phosphate oxygen coordinating the metal centre instead of one nitrogen from the macrocycle, either one secondary or the tertiary nitrogen, respectively. In Figure 7, these two possibilities are shown as three-dimensional molecular models, for which 172 and 167 kcal/mol potential energies were calculated, respectively.

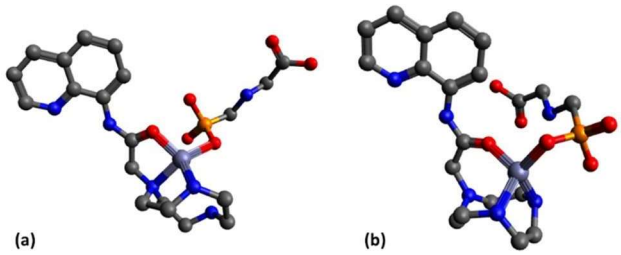

Figure 7. Three-dimensional model of two possible $[ZnL2]^{2+}$ adducts with glyphosate. One phosphate oxygen coordinates the metal centre instead of one nitrogen from the macrocycle, either (a) one secondary or (b) the tertiary nitrogen. Hydrogen atoms are not shown for the sake of clarity.

Subsequently, we investigated the potentialities of the Zn(II) complexes of the three ligands as fluorescent chemosensors for glyphosate.

At first, we performed a spectrofluorimetric screening of Zn(II) complexes of **L1**, **L2** and **L3** toward H_3PMG, H_2GLU, H_2AMPA, and phosphate. In the case of **L1**, the fluorescence emission of its Zn(II) complex at pH 7 was not influenced by the presence of the analytes, even in large excess (10 equiv.), as shown in Figure S7 (ESI†).

In the case of Zn(II) complexes with **L2** and **L3**, a significant quenching of the fluorescence intensity, ON-OFF response, was observed only upon addition of H_3PMG at pH 7 (Figure 8 and S8 for **L2** and **L3**, respectively, ESI†). The other analytes considered did not affect the emission ON state of $[ZnL2]^{2+}$, although we observed a decrease of the fluorescent emission for $[ZnL3]^{2+}$ complex also in the presence of H_2AMPA (Figure S8, ESI†).

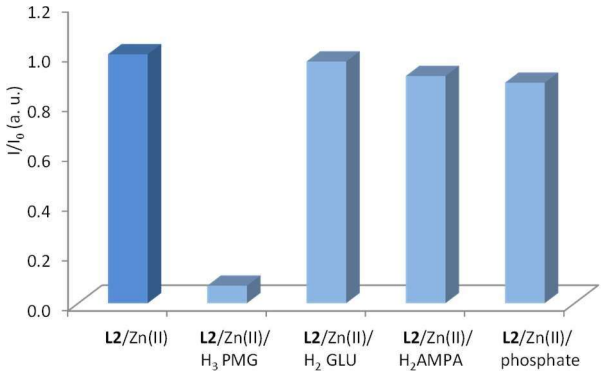

Figure 8. Normalized relative fluorescence emission intensity of the $[ZnL2]^{2+}$ complex upon addition of 10 equiv. of H_3PMG, H_2GLU, H_2AMPA and phosphate. ($[ZnL2]^{2+}$ = 2.52 × 10^{-5} M, MeCN/H_2O 1:4 v/v, pH 7, 298 K, λ_{exc} = 330 nm).

As previously shown by the ^{1}H NMR studies (Figure 6), the effect of H_3PMG is to weaken the interaction of the macrocyclic amine groups with the metal resulting in a photoinduced electron transfer (PET) effect.

Fluorescence titration experiments were then carried out by adding a H_3PMG aqueous solution to the $[ZnL]^{2+}$ (**L** = **L2** and **L3**) complexes in MeCN/H_2O (1:4 v/v) at pH 7. As shown in Figure 9, with the increase of the concentration of glyphosate, the fluorescence intensity of the probing system shows a significant decrease of the emission at 505 nm (λ_{exc} = 330 nm). Considering the $[ZnL2]^{2+}$ system, the minimum of fluorescence intensity is reached at a $[H_3PMG]/[ZnL2]^{2+}$ molar ratio of 8 and was approximately 20-fold lower than that of the solution without glyphosate, while for $[ZnL3]^{2+}$ the $[H_3PMG]/[ZnL3]^{2+}$ molar ratio necessary to reach the minimum of the fluorescence intensity emission is about 6 and the decrease of fluorescence is approximately 10-fold lower.

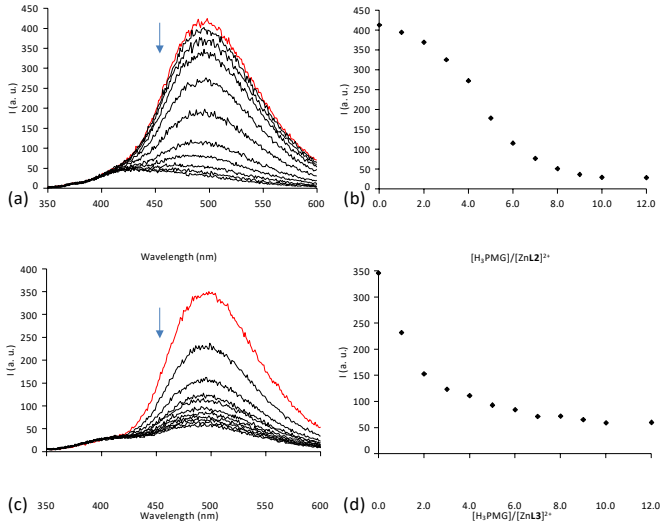

Figure 9. Fluorescence emission spectra (a) and (c) and emission intensity at 505 nm of $[ZnL2]^{2+}$ (b) and $[ZnL3]^{2+}$ (d), upon addition of increasing amounts of H_3PMG. ([**L2**] = 2.52 × 10^{-5} M, [**L3**] = 2.13 × 10^{-5} M, MeCN/H_2O (1:4 v/v), pH 7, 298 K, λ_{exc} = 330 nm).

We also analyzed possible interfering effects of the other analytes on the emission of the **L2**/Zn(II)/H_3PMG system. When H_3PMG (10 equiv.) was added to the solution containing 20 equiv. of the other substrates (H_2AMPA, H_2GLU and phosphate), a quenching of the fluorescence emission was observed, indicating that these species do not interfere with the detection of glyphosate. The results of the competitive experiments indicate that H_2AMPA, H_2GLU and phosphate do not affect the detection of H_3PMG by the **L2**/Zn(II) system (Figure S9, ESI†).

Test paper for sensing glyphosate.

A possible application of the $[ZnL2]^{2+}$ complex as sensor for H_3PMG can be evaluated by a test strip. For this purpose, the neutral filter paper was immersed in a MeCN/H_2O 1:4 v/v solution of **L2** (10^{-4} M) at pH 7 for 3 minutes to prepare a **L2** sensing test paper. After drying at room temperature, the obtained test paper was cut into circular portions and three drops of 10^{-4} M solution of $Zn(ClO_4)_2{\cdot}6H_2O$ were added to each of them. As shown in Figure 10, by adding to the test papers three drops of 10^{-4} M water solution of H_3PMG, H_2GLU, H_2AMPA or $CaHPO_4$, the quenching of the fluorescence emission was observed only in the presence of H_3PMG (test paper 3 in the Figure 10), while no significant fluorescence emission change was observed upon addition of the other considered species. These results point out the good ability of the $[ZnL2]^{2+}$ complex-based test paper for detection of H_3PMG.

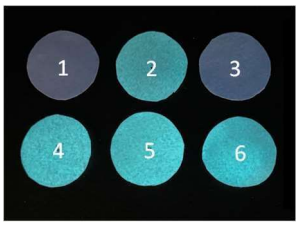

Figure 10. Fluorescence photographs (under UV_{365} light) of test papers containing the $[ZnL2]^{2+}$ complex upon addition of the different analytes: 1 = **L2**, 2 = $[ZnL2]^{2+}$, 3 = $[ZnL2]^{2+}$ + H_3PMG, 4 = $[ZnL2]^{2+}$ + H_2GLU, 5 = $[ZnL2]^{2+}$ + H_2AMPA, 6 = $[ZnL2]^{2+}$ + $CaHPO_4$.

Experimental

Instruments and Materials. ^1H- and proton-decoupled ^{31}P spectra were acquired at 298 K using a Bruker Avance III HD 600 MHz spectrometer, and peak positions are reported relative to tetramethylsilane (SiMe4). ^1H NMR titrations of the **L2** were performed by adding to a solution of the ligand (4.56 × 10^{-3} M, 0.7 mL), a solution of $Zn(ClO_4)_2{\cdot}6H_2O$ in CD_3CN to obtain a **L2**/M 1:1 molar ratio. To the resulting solution increasing volumes of a solution of H_3PMG in D_2O were added. Absorption and fluorescence spectra were registered on a Perkin-Elmer Lambda 6 spectrophotometer and on a Perkin-Elmer LS55 spectrofluorimeter, respectively for **L1** and Thermo Nicolet Evolution 300 spectrophotometer with a Varian Cary Eclipse fluorescence spectrophotometer for **L2** and **L3**. All measurements were performed at 298.0 ± 0.1 K. For spectrophotometer measurements, MeCN (Uvasol, Merck) and Millipore grade water were used as solvents. Spectrofluorimetric titrations of the **L2** and **L3** were performed by adding to a solution of the ligand (2.13 × 10^{-5}–2.52 × 10^{-5} M in MeCN/H_2O (1:4 v/v), 3 mL), a solution of $Zn(ClO_4)_2{\cdot}6H_2O$ in MeCN, to obtain a **L**/M 1:1 molar ratio. To the resulting solution increasing volumes of a solution of substrates in water (H_3PMG, H_2AMPA, H_2GLU, $CaHPO_4$) were added. The ESI mass study was performed using a TripleTOF® 5600+ high-resolution mass spectrometer (Sciex, Framingham, MA, U.S.A.), equipped with a DuoSpray® interface operating with an ESI probe. Respective ESI mass spectra were acquired through direct infusion at 7 µL/min flow rate. Stock solutions 10^{-5} M of the compounds were prepared in MeCN/H_2O (1:4 v/v).

Molecular potential energy was obtained by Marvin[47] through the conformers search tool. The Dreiding force field was selected with 0.1 kcal/mol diversity criteria among different conformers. 100 conformers were calculated and the one with the lowest potential energy was selected.

Solvents for other purposes and starting materials were purchased from commercial sources where available. **L1**,[39] **L2**[38] and **L3**[37a] were prepared by published methods.

Synthesis of $[ZnL1](ClO_4)_2{\cdot}0.25H_2O$.

An solution of $Zn(ClO_4)_2{\cdot}6H_2O$ (13 mg, 0.05 mmol) in H_2O (5 mL) was slowly added to a solution of **L1** (16 mg, 0.05 mmol) in H_2O (10 mL). The pH of the solution was adjusted to 7 by addition of a small amount of an aqueous solution of NaOH 0.1 M. Evaporation at room temperature of the resulting solution produced colorless crystals of $ZnL1](ClO_4)_2{\cdot}0.25H_2O$, which were filtered off and dried in vacuum. Yield 8 mg., 27%. Anal. elem. calcd for $C_{18}H_{28}Cl_2N_5O_{8.5}Zn$: C, 36.85; H, 4.81; N, 11.94. Found: C, 36.7; H, 4.9; N, 11.9.

Potentiometric measurements. All pH measurements (pH = −log [H^+]) employed for the determination of the constants for ligand

protonation, metal complex stability and formation of the ternary adducts were carried out in 0.10 M NMe_4Cl MeCN/H_2O (1:4 v/v) solution at 298.1 ± 0.1 K by means of conventional titration experiments under an inert atmosphere. The equipment and procedure used has been previously described.[48] The standard potential $E°$ and the ionic product of water (pK_w = 14.99(1) at 298.1 ± 0.1 K in 0.10 M NMe_4Cl) were determined by Gran's method.[49] At least three measurements (with about 100 data points for each) were performed for each system. In all experiments the ligand concentration [**L**] was about 1×10^{-3} M. In the complexation experiments the metal ion concentration was generally 0.9×0^{-3} M, while the concentration of the substrates (H_3PMG, H_2AMPA, H_2GLU, and phosphate) was varied for 0.5 to 5×10^{-3} M. The computer program HYPERQUAD[50] was used to calculate the equilibrium constants from emf data.

X-ray Crystallography.

X-ray diffraction data for compound [Zn**L1**]$(ClO_4)_2 \cdot 0.25H_2O$ were collected on an Oxford Diffraction Excalibur diffractometer using a Cu Kα radiation (λ = 1.54178 Å). Data collection was performed at 100 K. The program CrysAlis v 1.171[51] was used to determine the cell parameters, to collect the intensity data and to reduce them. Intensities were corrected for Lorentz and polarization effect. Absorption correction was performed with the program ABSPACK implemented in CrysAlis.

The structure of [Zn**L1**]$(ClO_4)_2 \cdot 0.25H_2O$ was solved by using the SIR-2004 package[52] and subsequently refined on the F2 values by the full-matrix least-squares program SHELXL-2014.[53] All the non-hydrogen atoms were anisotropically refined while all the hydrogen ones, with the exception of those of the water molecule that were not introduced in the refinement, were set in calculated position and refined in accordance with the atom to which they are bound. The two perchlorate anions were in disordered position, for one of these the disorder was modelled by using two positions for all the atoms (occupancy factors were refined to values of 0.59105 and 0.40895, for Cl2O21-O24 and Cl3O31-O34 respectively) for the other anion only the oxygen atoms were put in double position with an occupancy factor of 0.63025 and 0.36975 for O11-14 and O15-O18, respectively. Geometrical calculations were performed by PARST97[54] and molecular plots were produced by the Mercury 2.4 program.[55] Crystallographic data and refinement parameters are reported in Table S3 in the ESI†.

Conclusions

The binding and sensing ability of the Zn(II) complexes with **L1**, **L2** and **L3** towards phosphate-based anionic pollutants (fromtwo widely used pesticides, like glyphosate and glufosinate, to simple phosphate) is strictly related to the coordination sphere of the metal center. In fact, the Zn(II) complex with **L2**, in which the metal displays a coordination environment poorly saturated by the ligand donors, results the best receptors for all substrates, while the [Zn**L1**]$^{2+}$ complex, which contains a metal ion firmly bound by five nitrogen donor atoms, is the less efficient receptor. Among the different substrates, H_3PMG is selectively bound over the other analytes by [Zn**L2**]$^{2+}$. This selectivity is lost in the case of [Zn**L1**]$^{2+}$, which shows similar affinity for H_3PMG and H_2GLU. In all case, however, H_2AMPA and phosphate give the weakest interactions with the metal complexes. Interestingly, only in the case of [Zn**L2**]$^{2+}$ with $HPMG^{2-}$ there is a wide pH window in which the ternary species [Zn**L2**(HPMG)] is the prevailing specie present in solution including neutral pH. ^{1}H NMR titrations further supported the interaction of H_3PMG with the Zn(II) complex of **L2**. In fact, the signals of the [Zn**L2**]$^{2+}$ complex are affected by the formation of the adduct with this substrate, indicating a likely interaction of the phosphate group of glyphosate with the metal center as also supported by ^{31}P NMR studies. The fluorescence sensing ability of the complexes parallels their binding efficiency. H_3PMG is specifically signalled over the other substrate by the [Zn**L2**]$^{2+}$ complex, whose emission is dramatically quenched in the presence of this analytes. Selective sensing is partially lost in the case of [Zn**L3**]$^{2+}$, in which the quenching effect is less marked and it is also given by H_2AMPA. Finally, the test strip alsoshowed a good ability of the [Zn**L2**]$^{2+}$ complex-based test paper for the selective detection of H_3PMG over the other analytes considered. This system is a rare example of a metal based fluorescent probe able to recognize and detect efficiently glyphosate over other anionic substrates via a Chelation Quenching of the Fluorescence Emission (CHQF effect). In fact, as compared to a similar system containing a Zn(II)-dinuclear complex, our Zn(II) complex exhibits a higher formation constant with glyphosate.

These results here reported clearly point out that metal complex hosts represent a good choice for the development of optical probes capable of recognizing/sensing anionic target species in aqueous solution *via* covalent interactions at the metal center of the guests. The structural features of metal-complex receptors in terms of nature of the metal ion, supporting ligand and coordination sphere at the metal center are all crucial points to consider carefully and that require fine tuning for the design of efficient metal-based optical probes.

Conflicts of interest

There are no conflicts to declare.

Acknowledgements

The authors thank MIUR (PRIN 2017 2017EKCS35 project) and Fondazione di Sardegna (FdS Progetti biennali di Ateneo, annualità 2018 and 2020) for financial support and CeSAR (Centro Servizi d'Ateneo per la Ricerca) of the University of Cagliari, Italy, for NMR experiments. The authors also thank Mr. Riccardo Atzei for his collaboration.

References

1 a) A. Székács, B. Darvas, InTech, Rijeka, 2012, 247–284; b) A. Székács, B. Darvas, *Front. Environ. Sci.*, 2018, **6**, article 78; c) J. G. Zaller, *Springer Nature*, Cham., 2020.

2 J. G. Zaller, M. Weber, M. Maderthaner, E. Gruber, E. Takács, M. Mörtl, S. Klátyik, J. Győri, J. Römbke, F. Leisch, B. Spangl, A. Székács, *Environ. Sci. Eur.*, 2021**, 33**, Article 51.

3 J. J-L´opez, E.J. L-Martínez, P. O-Barrales, A. R-Medina, *Talanta*, 2020, **207**, 120344.

4 K.A. Rawat, R.P. Majithiya, J.V. Rohit, H. Basu, R.K. Singhal, S.K. Kailasa, *RSC Adv.*, 2016, **6**, 47741–47752.

5 C. F. B. Coutinho, L. F. M. Coutinho, L. H. Mazo, S. L. Nixdorf, C. A. P. Camara, F. M. Lancas, *Anal. Chim*. Acta, 2007, **592**, 30–35.
6 E. De Clercq, *Biochem. Pharmacol*., 2011, 82, 99–109.
7 Y.-C. Chang, Y.-S. Lin, G.-T. Xiao, T.-C. Chiu, C.-C. Hu, *Talanta,* 2016, **161**, 94–98.
8 A. Grandcoin, S. Piel, E. Baures, *Water Research,* 2017, **117**, 187-197.
9 X. Wang, M. Sakinati, Y. Yang, Y. Ma, M. Yang, H. Luo, C. Hou, D. Huo, *Anal. Methods,* 2020, **12**, 520–527.
10 M. Gui, J. Jiang, X. Wang, Y. Yan, S. Li, X. Xiao, T. Liu, T. Liu, Y. Feng, *Sensor. Actuator. B Chem*., 2017, **243**, 696–703.
11 H. Liu, P. Chen, Z. Liu, J. Liu, J. Yi, F. Xia, C. Zhou, *Sensor. Actuator. B Chem*., 2020, **304**, 127364.
12 a) K. Z. Guyton, D. Loomis, Y. Grosse, F. El Ghissassi, L. Benbrahim-Tallaa, N. Guha, K. Straif, *The Lancet Oncol.*, 2015, **16**(5), 490–491); b) F. Meloni, G. Satta, M. Padoan, A. Montagna, I. Pilia, A. Argiolas, S. Piro, C. Magnani, A. Gambelunghe, G. Muzi, G. M. Ferri, L. Vimercati, R. Zanotti, A. Scarpa, M. Zucca, S. De Matteis, M. Campagna, L. Miligi, P. Cocco, *Environ. Health*, 2021, 20:49, 1-8.
13 a) C.M. Benbrook, *Environ. Sci. Eur*., 2019, **31**, 2-16; b) F. Qu, H. Wang, J. You, *Food Chem*., 2020, **323**, 126815; c) J. Zheng, H. Zhang, J. Qu, Q. Zhu, X. Chen, *Anal. Methods*, 2013, **5**, 917-924.
14 X. Ding, K.-L. Yang, *Anal. Chem*., 2013, **85**, 5727–5733.
15 H. K. Takano, F. E. Dayan, *Pest. Manag. Sci.*, 2020, **76**, 3911-3925.
16 H. K. Takano, R. Beffa, C. Preston, P. Westra, F. E. Dayan, *Photosynth. Res.* 2020, **144**, 361–372).
17 R. C. Lajmanovich, A. M. Attademo, G. Lener, A. P. Cuzziol Boccioni, P. M. Peltzer, C. S. Martinuzzi, L. D. Demonte, M R. Repetti. *Sci., Total Environ*., 2022, **804**, 150177.
18 M.V. Khrolenko, P.P. Wieczorek, *J. Chromatogr. A*, 2005, **1093**, 111–117.
19 Y. Sun, C. Wang, Q. Wen, G. Wang, H. Wang, Q. Qu, X. Hu, *Chromatographia,* 2010, **72**, 679–686.
20 T. Saito, H. Aoki, A. Namera, H. Oikawa, S. Miyazaki, A. Nakamoto, S. Inokuchi, *Anal. Sci.*, 2011, **27**, 999–1005.
21 Y. Zhu, F.F. Zhang, C.L. Tong, W.P. Liu, *J. Chromatogr. A*, 1999, **850**, 297–301.
22 E. Orejuela, M. Silva, *Electrophoresis*, 2005, **26**, 4478–4485.
23 D. Wang, B. Lin, Y. Cao, M. Guo, Y. Yu, J. Agric. Food Chem., 2016, **64**, 6042–6050.
24 M. Á. González-Martínez, E.M. Brun, R. Puchades, Á. Maquieira, K. Ramsey, F. Rubio, *Anal. Chem*., 2005, **77**(13), 4219–4227.
25 F. Bettazzi, A. Romero-Natale, E. Torres, I. Palchetti, *Sensors*, 2018, 18(9), 2965.
26 E. C. Reynoso, R.D. Peña, D. Reyes, Y. Chavarin-Pineda, I. Palchetti, E. Torres, *Int. J. Environ. Res. Public Health,* 2020, **17**(19), 7102.
27 V. Narayanan, D.S. Prasad, *Biosens. Bioelectron*., 2020, **170**, 112609.28 a) C. Y. Hong, S. S. Ye, C. Y. Dai, C. Y. Wu, L. L. Chen, Z. Y. Huang, *Anal. Bioanal. Chem*. 2020, **412**, 8177−8184; b) B. J. Lv, M. Wei, Y. J. Liu, X. Liu, W. Wei, S. Q. Liu, *Microchim. Acta* 2016, **183**, 2941−2948;
c) X. Yan, H. X. Li, T. Y. Hu, X. G. Su, *Biosens. Bioelectron*. 2017, **91**, 232−237; d) X. Yan, Y. Song, C. Z. Zhu, H. X. Li, D. Du, X. G. Su, Y. H. Lin, *Anal. Chem*., 2018, **90**, 2618−2624; e) L. Yang, Y. L. Liu,
C. G Liu, F. Ye, Y. Fu, *J. Hazard. Mater*., 2020, **381**, No. 120966; f) X. F. Wang, M. Sakinati, Y. X. Yang, Y. Ma, M. Yang, H. B. Luo, C. J. Hou, D. Huo, *Anal. Methods,* 2020, **12**, 520−527. 29 a) J. Guan, J. Yang, Y. Zhang, X. Zhang, H. Deng, J. Xu, J. Wang, M.-S. Yuan, *Talanta*, 2021, **224**, 121834; b) F. Sun, L. Yang, S. Li, Y. Wang, L. Wang, P. Li, F. Ye, Y, Fu, *J. Agric. Food Chem*., 2021, **69**, 12661−12673; c) L. Conti, N. Flore, M. Formica, L. Giorgi, M. Pagliai, L. Mancini, V. Fusi, B. Valtancoli, C. Giorgi, *Inorg. Chim. Acta*, 2021, **519**, 120261.
30 J. Zhao, D. Yang, X. J. Yang, B. Wu, *Coord. Chem. Rev*., 2019, **378**, 415–444.
31 P.A. Gale, E.N.W. Howe, X. Wu, M.J. Spooner, *Coord. Chem. Rev*., 2018, **375**, 333–372.
32 R. Martínez-Mannez, F. Sancenon, *J. Fluoresc.*, 2005, **15**, 267–285.
33 A. Patil, S. Salunke-Gawali, *Inorg. Chim. Acta*., 2018, **482**, 99–112.
34 D. Wu, A.C. Sedgwick, T. Gunnlaugsson, E.U. Akkaya, J. Yoon, T.D. James, *Chem. Soc. Rev*., 2017, **46**, 7105–7123.
35 C. Bazzicalupi, A. Bencini, V. Lippolis, *Chem. Soc. Rev*., 2010, **39**, 3709-3728.
36 A. Bencini, V. Lippolis, B. Valtancoli, *Inorg. Chim. Acta*, 2014, **417**, 38-58.
37 a) A. Garau, A. Bencini, A. J. Blake, C. Caltagirone, L. Conti, F. Isaia, V. Lippolis, R. Montis, P. Mariani, M. A. Scorciapino, *Dalton Trans*. 2019, **48**, 4949-4960; b) C. Caltagirone, A. Bencini, F. Caddeo, A. Garau, M.B. Husthouse, F. Isaia, S. Lampis, V. Lippolis, V. Meli, M. Monduzzi, M.C. Mostallino, S. Murgia, S. Puccioni, F. Lopez, P.P. Secci, Y. Taalmon, J. Schmidt, *Org. Biomol. Chem.* 2013, **11**, 7751-7759; c) C. Bazzicalupi, A. Bencini, A. Bianchi, A. Danesi, C. Giorgi, C. Lodeiro, F. Pina, S. Santarelli, B. Valtancoli, *Chem. Commun.* 2005, 2630– 2632; d) A. Bencini, V. Lippolis, *Coord. Chem. Rev.* 2020, **407**, 213151.
38 A. Garau, M. C. Aragoni, M. Arca, A. Bencini, A. J. Blake, C. Caltagirone, C. Giorgi, V. Lippolis, M. A. Scorciapino, *ChemPlusChem.*, 2020, **85**, 1789-1799.
39 F. Bartoli, L. Conti, G. M. Romano, L. Massai, P. Paoli, P. Rossi, G. Pietraperzia, C. Gellini, A. Bencini, *New J. Chem.***,** 2021, **45**, 16926-16938.
40 E. Kimura, H. Kitamura, T. Koike, M. Shiro, *J. Am. Chem. Soc*., 1997, **119**, 10909-10919.
41 I. Freuze, A. Jadas-Hecart, A. Royer, P.-Y. Communal, *J. Chromatogr*. *A*, 2007, **1175**, 197-206.
42 D. A. Martinez, U. E. Loening, M. C. Graham, *Environ. Sci. Eur*. 2018, 30:2.
43 M. S. Caetano, T. C. Ramalho, D. F. Botrel, E. F. F. da Cunha, W. C. de Mello, *Int. J. Quantum Chem.* 2012, **112**, 2752–2762.
44 B. Liu, L. Dong, Q. Yu, X. Li, F. Wu, Z. Tan, S. Luo, *Phys. Chem. B,* 2016, **120**, 2132–2137.
45 Q. Li, B. Liu, W. Mu, Q. Yu, Y. Tian, G. Liu, Y. Yang, X. Li, S. Luo, *J. Sol. Chem.*, 2018, **47**, 705–714.
46 A. Bianchi, E. Garcia-España, *J. Chem. Educ.* 1999, **76**, 1727– 1732.
47 *MarvinSketch (vol. 15.7.13.0)*; ChemAxon, 2015.
48 A. Bencini, A. Bianchi, M. Micheloni, P. Paoletti, E. Garcia-España, M. A. Niño**,** *J. Chem. Soc., Dalton Trans.***,** 1991, 1171-1174.
49 G. Gran, *Analyst* (London) 1952, **77**, 661-671.
50 P. Gans, A. Sabatini, A. Vacca, *Talanta,* 1996, **43**, 1739-1753.
51 CrysAlisPro 1.171.38.41r (Rigaku Oxford Diffraction, 2015)
52 M. C. Burla, R. Caliandro, M. Camalli, B. Carrozzini, G. L. Cascarano, L. De Caro, C. Giacovazzo, G. Polidori, R. Spagna*, J. Appl. Cryst*., 2005, **38**, 381–388.
53 G.M. Sheldrick, *Acta Cryst*., 2015, **C71**, 3–8.
54 M. Nardelli, *J. Appl. Cryst*., 1995, **28**, 659-662.
55 C. F. Macrae, I. J. Bruno, J. A. Chisholm, P. R. Edgington, P. McCabe, E. Pidcock, L. Rodriguez-Monge, R. Taylor, J. van de Streek, P. A. Wood, *J. Appl. Cryst*., 2008, **41**, 466-470.